Adsorption of marine phycotoxin okadaic acid on a covalent organic framework

Laura M. Salonen [a], Sara R. Pinela [a,b], Soraia P.S. Fernandes [a], João Louçano [a],
Enrique Carbó-Argibay [a], Marisa P. Sarriá [a], Carlos Rodríguez-Abreu [a,1], João Peixoto [b],
Begoña Espiña [a,*]

[a] *International Iberian Nanotechnology Laboratory (INL), Av. Mestre José Veiga s/n, 4715-330 Braga, Portugal*
[b] *CEB – Centre of Biological Engineering, University of Minho, 4710-057 Braga, Portugal*

ARTICLE INFO

ABSTRACT

Phycotoxins, compounds produced by some marine microalgal species, can reach high concentrations in the sea when a massive proliferation occurs, the so-called harmful algal bloom. These compounds are especially dangerous to human health when concentrated in the digestive glands of seafood. In order to generate an early warning system to alert for approaching toxic outbreaks, it is very important to improve monitoring methods of phycotoxins in aquatic ecosystems. Solid-phase adsorption toxin tracking devices reported thus far based on polymeric resins have not been able to provide an efficient harmful algal bloom prediction system due to their low adsorption capabilities.

In this work, a water-stable covalent organic framework (COF) was evaluated as adsorbent for the hydrophobic toxin okadaic acid, one of the most relevant marine toxins and the parental compound of the most common group of toxins responsible for the diarrhetic shellfish poisoning. Adsorption kinetics of okadaic acid onto the COF in seawater showed that equilibrium concentration was reached in only 60 min, with a maximum experimental adsorption of 61 mg g^{-1}. Desorption of okadaic acid from the COF was successful with both 70% ethanol and acetonitrile as solvent, and the COF material could be reused with minor losses in adsorption capacity for three cycles. The results demonstrate that COF materials are promising candidates for solid-phase adsorption in water monitoring devices.

© 2017 Elsevier B.V. All rights reserved.

1. Introduction

Microalgae in marine environment and cyanobacteria in both marine and freshwater ecosystems can produce harmful effects, including a broad range of phenomena referred to as harmful algal blooms (HABs). During some HABs high amounts of toxins are produced, which can accumulate in the flesh of seafood, and more frequently in the digestive glands, implying large economic losses to seafood aquaculture. The occurrence of HABs is a general threat to human health worldwide [1], and effective early monitoring should be performed to allow the aquaculture industry to overcome the losses derived thereof, to improve human safety, and to obtain more knowledge of HAB dynamics in a climate-change scenario.

Diarrhetic shellfish poisoning (DSP) is a foodborne intoxication caused by ingestion of shellfish such as mussels, scallops, oysters, or clams contaminated with DSP toxins, including the okadaic acid (OA) group of toxins as the most representative of them. In a toxic OA outbreak only low concentration of the toxin can be found in the marine environment due to its limited stability in seawater and due to the fact that a great part of the toxin is retained inside the producer microalgae [2]. Thus, seawater sampling methods that efficiently concentrate OA are required in order to be able to predict a toxic episode in seafood before the concentration of OA reaches the maximum concentration allowed in legislation [3].

In the last decade, new adsorption techniques have been developed and implemented for passive *in situ* concentration of contaminants present in water for posterior analysis in the laboratory. Polar organic chemical integrative samplers, consisting of a sequestration medium enclosed within hydrophilic microporous polyethersulfone membranes, have been successfully used to sample polar organic chemicals in aquatic environments [4,5]. Other kind of semi-permeable membrane devices have been used

for the monitoring of polycyclic aromatic hydrocarbons [6]. For microalgae-produced toxins, passive solid-phase adsorption toxin tracking (SPATT) systems have been studied and their usefulness has been demonstrated in concentrating hydrophobic toxins such as okadaic acid, pectenotoxins, azaspiracids, dinophysistoxins, and yessotoxins [7]. The SPATT system consists of batches of previously hydrated adsorbent resins within a polyester mesh, sown with polyester thread. The bags are installed in a frame attached to a weighted line at different locations and depths [2].

The nature, properties, and behavior of the solid-phase adsorbent are the major challenges in the development of SPATT devices. Several polymeric resins have been investigated but the best results in terms of adsorption and desorption rates have been obtained with resins based on a styrene–divinylbenzene matrix, such as Diaion HP-20, Sepabeads SP850, and Sepabeads SP825L [7]. HP-20, so far the best performing resin for adsorption of the OA group of toxins, was found to adsorb a maximum of 1639 μg g^{-1} of OA [8]. A recent study showed that HP-20 SPATT devices allowed the detection of toxins in a similar time frame than when detected in shellfish tissues by LC–MS analyses in regulatory centers [9]. However, in order to provide the aquaculture industry with a sufficiently efficient tool to remove the seafood from the seawater before contamination occurs, a prediction level of weeks is necessary. Thus, the development of more efficient adsorbents is essential to allow for the prediction of HABs sufficiently in advance, and to obtain a practical early warning system for DSP outbreaks in aquaculture sites.

Covalent organic frameworks (COFs) are crystalline porous materials formed by the self-assembly of purely organic building blocks [10–12]. These materials feature uniform pores in the micro- and mesoporous range, ranging from 1 to around 5 nm in diameter, the form and size of which can be tuned by the choice of building blocks. COFs are thermally stable and, with the appropriate choice of building blocks, can also show high stability under aqueous conditions [13,14]. The versatility of the structures and the high surface areas make them interesting adsorbents, and in recent reports COFs have shown promise for organic dye removal [15–18], as carriers for drug delivery [19–21], and isolation of industrially relevant compounds [22].

Herein, we demonstrate the efficiency of COFs in capturing OA from seawater. The results show promise for COF materials to be used as improved adsorbents in SPATT devices for HAB forecasting and monitoring.

2. Materials and methods

2.1. Materials

TpBD-Me$_2$ COF [14] was prepared according to the literature; for further details on the synthesis and characterization, see the Supporting Information (SI). A COF dispersion of 1 mg mL^{-1} in synthetic seawater was used in all experiments with OA.

Okadaic acid from *Prorocentrum* sp. was purchased from Merck-Calbiochem (Darmstadt, Germany), 6,8-difluoro-4-methylumbelliferyl phosphate (DiFMUP) from Molecular Probes (Eugene, USA), protein phosphatase-1 (PP1) catalytic subunit, α-isoform from rabbit, synthetic ASTM seawater, and all other reagents for the OA quantification were purchased from Sigma-Aldrich (Sintra, Portugal).

2.2. The stability of TpBD-Me$_2$ COF in aqueous medium

TpBD-Me$_2$ COF (16 mg) was suspended in ultrapure water or synthetic seawater (2.8 mL) at room temperature for 7 days. Then,

the samples were centrifuged (3000 RCF, 15 min, room temperature), and the aq. medium was removed.

The sample suspended in ultrapure water was soaked in acetone for 8 h, centrifuged (3000 RCF, 15 min, room temperature), and the solvent was decanted. The soaking was repeated 3 times in total. The sample was then dried at 120 °C at high vacuum for 9 h.

In order to remove salts, the sample suspended in synthetic seawater was first soaked in ultrapure water for 8 h, centrifuged (3000 RCF, 15 min, room temperature), and the solvent was decanted. The soaking was repeated 3 times in total. Thereafter, the sample was treated as the sample suspended in ultrapure water.

2.3. Adsorption kinetics

Samples were prepared as follows for each time point: two replicates of 100 μL of a TpBD-Me$_2$ COF dispersion of 1 mg mL^{-1} in synthetic seawater were spiked with an OA concentration of 10, 15, 50, and 100 μmol L^{-1} and incubated at 19 °C under constant shaking at 7 RCF. After 0.5, 60, 240, and 480 min of incubation, the sample for the corresponding time point was centrifuged at 21420 RCF during 15 min at 19 °C. The time used for centrifugation was added to the time points as time elapsed, resulting in time points of 15.5, 75, 255, and 495 min, respectively. Supernatants were collected and analyzed for OA quantification.

2.4. Freundlich isotherm

Freundlich equation was used to analyze the equilibrium adsorption isotherm. Freundlich equation is expressed as

$$lg \ q_e = lg \ K_F + \left(\frac{1}{n}\right) \times lg \ C_e \tag{1}$$

where q_e is the adsorbate concentration on the adsorbent in equilibrium (mg g^{-1}), C_e is the equilibrium concentration of adsorbate in solution (mg L^{-1}), and n and K_F are characteristic constants. K_F is an indicator of the adsorption capacity in the Freundlich theory. The adsorption kinetics is defined as favorable if $n > 1$, implying that the adsorption rate is fast or controllable, depending on the requirement of the particular application. The maximum adsorption capacity (q_m) can be calculated from the following equation

$$q_m = K_F C_0^{1/n} \tag{2}$$

where C_0 is the initial concentration of the adsorbate in solution (mg L^{-1}).

The Freundlich Eq. (1) showed a good fit to the experimental data in a moderate solute concentration range, and includes a constant that describes the heterogeneity of the surface of the adsorbent, $1/n$. Fitting the experimental results using the Langmuir model resulted in a very low correlation coefficient (data not shown).

2.5. Desorption assay

Desorption tests were carried out with pellets obtained after centrifugation at 21420 RCF during 15 min from adsorption assays with an OA concentration of 10 μmol L^{-1}. The pellets were suspended in 200 μL of 70% ethanol or acetonitrile and incubated overnight at 4 °C under constant shaking at 7 RCF. The samples were then centrifuged at 21420 RCF for 15 min at 19 °C. Supernatants were recovered and analyzed for OA.

2.6. Recycling tests

First, the adsorption assays were carried out with an OA concentration of 10 μmol L^{-1} in synthetic seawater during 4 h at 19 °C
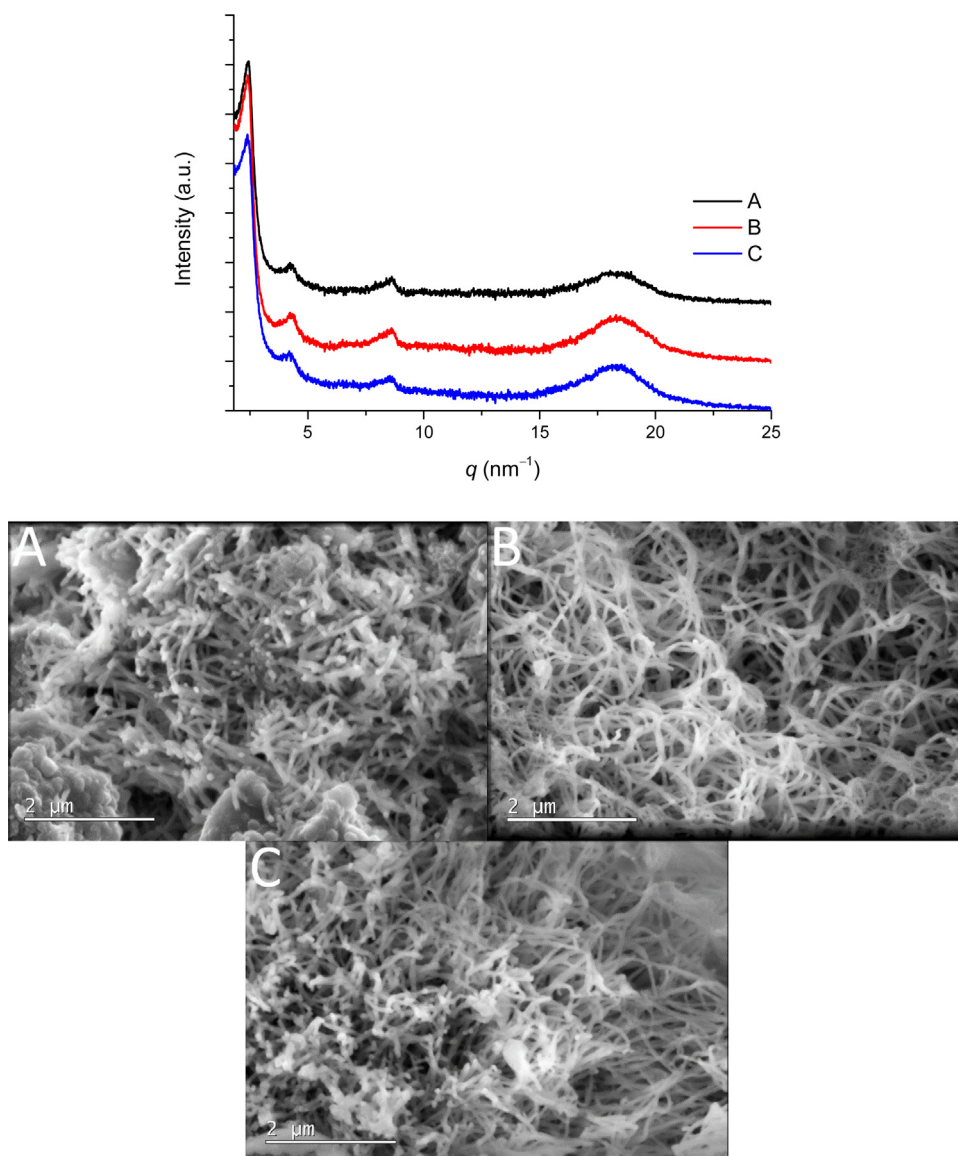
Fig. 1. A comparison of the SAXS data and SEM images before (A) and after soaking the COF for 7 days in ultrapure water (B) and synthetic seawater (C).

under constant shaking at 7 RCF. The samples were then centrifuged at 21420 RCF during 15 min at 19 °C. The supernatants were collected and OA was quantified (cycle 1). The pellets were re-suspended in ultrapure water and centrifuged at 21420 RCF during 15 min at 19 °C. The OA was desorbed from the pellets as indicated in 2.5. The pellets from desorption were re-suspended in synthetic seawater with an OA concentration of 10 μmol L^{-1}, initiating the adsorption cycle 2. The procedure was repeated for cycle 3.

2.7. Quantification of okadaic acid

The aqueous reaction buffer consists of 20 mM Tris-HCl, 5 mM MgCl$_2$, 1 mM MnCl$_2$, 1 mg mL^{-1} bovine serum albumin (BSA), and 0.1% 2-mercaptoethanol at pH = 8.

DiFMUP stock solution was prepared at 40 mM in Tris-HCl solution. OA stock solution was prepared at 1 mM in absolute ethanol and the one for PP1 at 3900 U mL^{-1} reconstituted from the lyophilized product with ultrapure water.

A separate calibration curve was used for each experiment of OA quantification, carried out in the same microplate as the rest of the samples. OA solutions for the calibration curves were prepared in the corresponding solvent, synthetic seawater for the quantifi-

cation of OA of the supernatants from the adsorption assays and acetonitrile or 70% ethanol for the quantification of OA of the supernatant from the desorption assays. For the calibration curves, see the SI Section 6.

PP1 inhibition assays were performed at a final volume of 200 μL in wells of flat-bottom opaque 96 well microplates. In short, first, 0.1 U of PP1 were added to the reaction wells containing 165 μL of reaction buffer. Afterwards, 20 μL of the corresponding solution of the OA calibration curve, solvent (blank), or supernatant samples from the adsorption/desorption assays were added to the well. The microplate was incubated during 30 min under constant shaking at 1 RCF at 37 °C for a maximum enzymatic inhibition. Then, 5 μL of DiFMUP solution (8 mM) was added to a final concentration of 200 μM. After 2 h under constant shaking at 1 RCF at 37 °C, fluorescence intensity was measured (excitation wavelength 315 nm, emission wavelength 470 nm) in a BioTek Synergy H1 microplate reader.

3. Results and discussion

As compared to the traditionally used macroporous resins, the use of COFs for toxin capture in SPATT devices can be advantageous
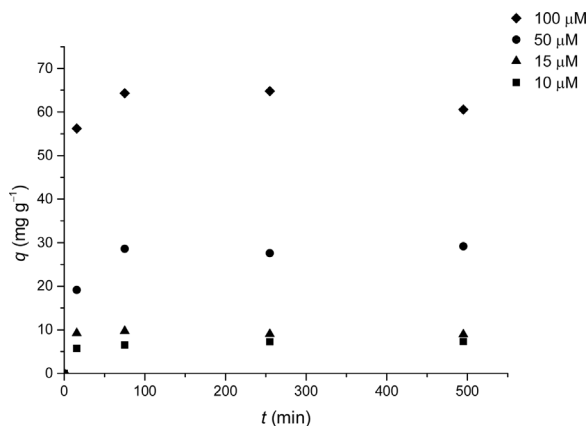
Fig. 2. Adsorption kinetic curves on TpBD-Me$_2$ COF for initial OA concentrations of 10, 15, 50, and 100 μmol L^{-1} at 19 °C.

not only due to the uniformity of the pores, but their small size as well, preventing the entry of large compounds and photosynthetic complexes present in the sea, such as chlorophyll pigments, into the adsorbent. This would facilitate the detection and quantification of the toxin from the samples by the approved analytical and functional methods, and result in obtaining cleaner concentrated extracts from the eluents of the adsorbent, leading to more accurate results. We chose TpBD-Me$_2$ COF [14] to be tested as an adsorbent for marine toxins due to its reported high stability in water, even under acidic or basic conditions. This stability is the result of the β-keto-enamine linkage [23], introduced to COFs by Banerjee and co-workers [13], which, due to an irreversible tautomerization step during the COF formation, also leads to materials with lower crystallinity as compared to boronic-acid-linked COFs. The surface area of TpBD-Me$_2$ COF is 468 m^2 g^{-1} [14], which is in the range of that of HP-20 [8], but the COF features a smaller pore diameter with ca. 2 nm as compared to the 10 nm reported for HP-20 [8]. Additionally, the hydrophobic nature of the pores with the methyl groups of the BD-Me$_2$ building block pointing into the cavity was expected to favor the adsorption of the hydrophobic OA. Interestingly, Banerjee and co-workers recently reported a solvent-free continuous synthetic procedure for the Tp-class of COFs [24], highlighting that these materials can be produced rapidly and on a large scale.

3.1. The stability of TpBD-Me$_2$ COF in aqueous medium

To allow the use of a material for SPATT applications, stability in seawater is necessary. The stability of TpBD-Me$_2$ COF was studied by soaking the material in both ultrapure water and synthetic seawater for seven days (for further details, see the experimental part). A comparison of the SAXS data before and after the aqueous treatment shows that the COF is stable under these conditions (Fig. 1), with the crystallinity retained even in the case of seawater. No noticeable morphological changes upon soaking can be seen in the scanning electron microscope (SEM) images, and the wire-like morphology dominates in all samples (Fig. 1, see also SI Section 7).

3.2. Adsorption kinetics

The kinetic curves show a fast adsorption phase during the first 60 min (Fig. 2), which can be explained by the large initial surface area available for adsorption [8]. Thereafter, the adsorption reaches equilibrium between adsorption and desorption due to the process dynamics, as seen by the flattening of the curve. For a constant temperature, a higher initial concentration of adsorbate is expected to imply a higher amount adsorbed [25], which is the case of OA adsorption onto the COF. The adsorption is almost instantaneous,
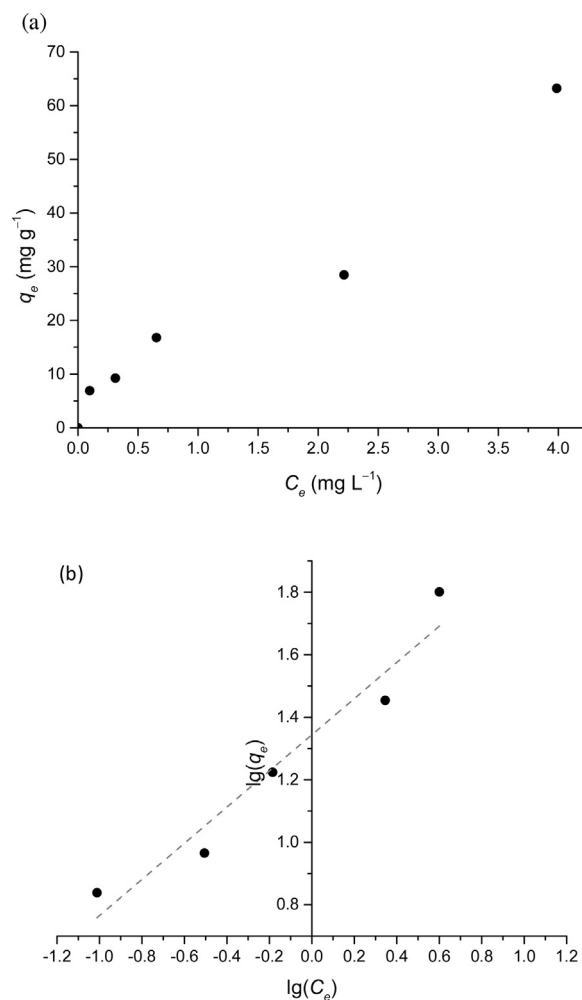

Fig. 3. a) Amount of OA adsorbed in equilibrium, q_e (mg g^{-1}), as a function of OA concentration in equilibrium, C_e (mg L^{-1}); b) linear regression of the Freundlich isotherm for the experimental adsorption of OA by TpBD-Me$_2$ COF.

Table 1
Freundlich isotherm equation constants and correlation coefficient derived from the graph in Fig. 3b.

Regression equation	lg q_e = (0.578 ± 0.089) lg C_e + (1.344 ± 0.049)
K_F (mg$^{1-1/n}$ g^{-1} L$^{1/n}$)	22.086 ± 1.1198
1/n	0.578 ± 0.082
n	1.729
R^2	0.92408

with ca. half of the equilibrium amount of OA adsorbed within the first 15 min.

Although the kinetic curves obtained in other studies on the adsorption of OA using chromatographic resins show the same profile as we observe for TpBD-Me$_2$ COF, adsorption equilibrium was reached at 225 min using the HP-20 resin [26], showing that adsorption to TpBD-Me$_2$ COF is very fast.

3.3. Isotherm at 19 °C

The adsorption isotherm at 19 °C was obtained by plotting the amount absorbed in equilibrium, q_e, against the concentration of OA in solution at equilibrium, C_e, as shown in Fig. 3a. The fitting of the experimental data to the Freundlich equation is shown in Fig. 3b. The values for K_F, 1/n, n, and R^2 are listed in Table 1, and were obtained by linear regression of the experimental values.
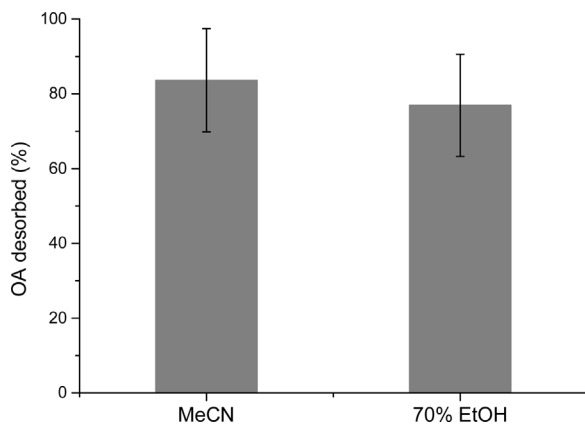
Fig. 4. Quantification of the OA desorption efficiency (%) as an average of three cycles from TpBD-Me$_2$ COF using 70% ethanol or acetonitrile as solvent after adsorption assays with 10 μM of OA and 100 μg of TpBD-Me$_2$ COF.

Fig. 5. Reusability of TpBD-Me$_2$ COF in consecutive cycles of OA adsorption/desorption with an OA concentration of 10 μM.

The Freundlich model is adequate to describe adsorption onto heterogeneous surfaces and at low initial concentrations of adsorbate. The constant n that reflects the degree of heterogeneity of the surface is higher than 1, indicating favorable adsorption.

K_F is an indicator of adsorption capacity, so that the higher the value of K_F, the higher the maximum adsorption capacity. This constant decreases with increasing temperature [25], and is also related to the strength of adsorbate–sorbent interaction [27]. We obtained a K_F value of 22.086 mg$^{0.422}$ g^{-1} L$^{0.578}$ for TpBD-Me$_2$ COF. For HP-20, K_F of 27.460 μg$^{0.112}$ g^{-1} L$^{0.888}$ was reported [8], with different n values hindering the comparison between the results [28].

The linear tendency of the isotherm indicates that the adsorbed amount is proportional to the equilibrium concentration of the solute in the solution. A linear isotherm is characteristic of homogeneous adsorbent surfaces and occurs at a low concentration. It also suggests that all the pores have the same affinity to OA [8]. Scarcity and high cost of the OA toxin standard prevented us from expanding the isotherm to higher concentrations to further confirm the applicability of the Freundlich model.

The previously reported maximum capacities for OA adsorption of 1.639 mg g^{-1} and 1.088 mg g^{-1} with the resins HP-20 and SP700, respectively, were calculated using equation 2 (see materials and methods section 2.4) [8], we obtained a value of 60.6 mg g^{-1} as the maximum amount of OA adsorbed when using the highest initial concentration of 100 μM, showing that TpBD-Me$_2$ COF can adsorb 38 times more OA than HP-20. Using equation 2, a maximum adsorption capacity (q_m) of 279 mg g^{-1} is obtained for TpBD-Me$_2$ COF, resulting in a 200-fold increase in comparison to previously reported values with styrene-based resins [8]. Although comparison between data is difficult due to differences in temperature, 19 °C in this study vs. 25 °C in the literature [8], with lower temperatures favoring adsorption, a higher efficiency in the case of the COF material as compared to the regularly used resins is demonstrated.

3.4. Desorption

In order to be able to use TpBD-Me$_2$ COF for OA monitoring, efficient desorption is of utmost importance. Both 70% ethanol and acetonitrile were tested as solvents for desorption due to their chemical compatibility with both OA and TpBD-Me$_2$ COF. As shown in Fig. 4, approximately 80% of the adsorbed OA can be recovered after a single incubation at 4 °C overnight in either of the solvents. However, desorption kinetic assays showed that equilibrium is reached after only 60 min of incubation with the solvents at 19 °C
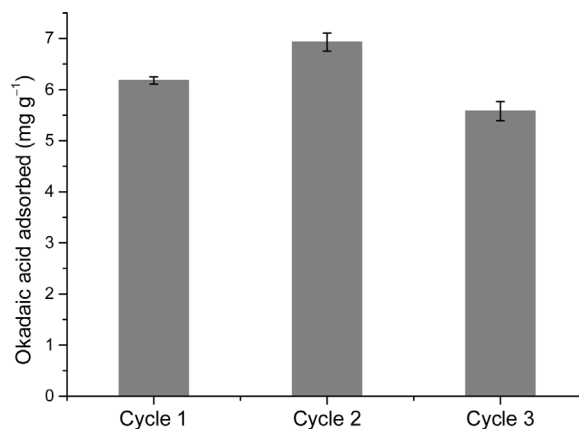
(see SI, figure SI8.1), highlighting the suitability of the COF material as adsorbent in the SPATT application.

3.5. Recycling

Very few reports exist on the regeneration of resins used for toxin adsorption [29], most probably due to the relatively low cost of the resins and the difficulties in performing cleaning efficiently. However, very recently, the need to develop nanocomposites as sorbents for SPATT and to investigate their regeneration to allow for their implementation in monitoring programs was underlined [30].

To reduce the cost of the material for the SPATT application, it is of interest to be able to use the adsorbent for various cycles, and therefore, the reusability of TpBD-Me$_2$ COF in consecutive cycles of OA adsorption/desorption was studied with an OA concentration of 10 μM. As observed in Fig. 5, the amount of OA adsorbed by the COF remained stable at around 6 mg g^{-1} in the first two cycles and was reduced to around 5.5 mg g^{-1} in the third, indicating a reduction in efficiency of merely 8%.

4. Conclusions

This study shows for the first time the potential of COFs as efficient adsorbents for toxins in seawater. TpBD-Me$_2$ COF shows unprecedented performance in OA adsorption, as evidenced by the fast OA adsorption kinetics and the values for K_F and n constants obtained from the Freundlich isotherm in seawater. Additionally, OA was easily and efficiently desorbed from the COF, allowing the reuse of the material for at least 3 cycles. Consequently, TpBD-Me$_2$ COF is a promising new adsorbent to be used in SPATT devices for the *in situ* concentration of OA dissolved in seawater to predict toxic outbreaks in seafood.

Further studies with different toxin mixtures, TpBD-Me$_2$ COF encapsulated in SPATT devices, and on-field tests are currently underway in our laboratories in order to explore the potential of this novel material for HAB monitoring.

Programme for research, technological development and demonstration under grant agreement no. 600375.

Appendix A. Supplementary data

References

[1] UNESCO, Manual on Harmful Marine Microalgae, UNESCO, Publishing, Paris, 2004 http://unesdoc.unesco.org/images/0013/001317/131711e.pdf.

[2] L. MacKenzie, V. Beuzenberg, P. Holland, P. McNabb, A. Selwood, Solid phase adsorption toxin tracking (SPATT): a new monitoring tool that simulates the biotoxin contamination of filter feeding bivalves, Toxicon 44 (2004) 901–918, http://dx.doi.org/10.1016/j.toxicon.2004.08.020.

[3] E. Union, REGULATION (EC) No 853/2004 OF THE EUROPEAN PARLIAMENT AND OF THE COUNCIL of 29 april 2004 laying down specific hygiene rules for food of animal origin, Off. J. Eur. Union. L 139 (2004) 69–74.

[4] D.A. Alvarez, J.D. Petty, J.N. Huckins, T.L. Jones-Lepp, D.T. Getting, J.P. Goddard, S.E. Manahan, Development of a passive, in situ, integrative sampler for hydrophilic organic contaminants in aquatic environments, Environ. Toxicol. Chem. 23 (2004) 1640–1648 http://www.ncbi.nlm.nih.gov/pubmed/15230316.

[5] M.J. Martínez Bueno, M.D. Hernando, A. Agüera, A.R. Fernández-Alba, Application of passive sampling devices for screening of micro-pollutants in marine aquaculture using LC–MS/MS, Talanta 77 (2009) 1518–1527, http://dx.doi.org/10.1016/j.talanta.2008.09.047.

[6] P.D. Boehm, D.S. Page, J.S. Brown, J.M. Neff, A.E. Bence, Comparison of mussels and semi-permeable membrane devices as inter-tidal monitors of polycyclic aromatic hydrocarbons at oil spill sites, Mar. Pollut. Bull. 50 (2005) 740–750, http://dx.doi.org/10.1016/j.marpolbul.2005.09.022.

[7] L.A. MacKenzie, In situ passive solid-phase adsorption of micro-algal biotoxins as a monitoring tool, Curr. Opin. Biotechnol. 21 (2010) 326–331, http://dx.doi.org/10.1016/j.copbio.2010.01.013.

[8] A. Li, F. Ma, X. Song, R. Yu, Dynamic adsorption of diarrhetic shellfish poisoning (DSP) toxins in passive sampling relates to pore size distribution of aromatic adsorbent, J. Chromatogr. A 1218 (2011) 1437–1442, http://dx.doi.org/10.1016/j.chroma.2011.01.043.

[9] G. Pizarro, Á. Moroño, B. Paz, J.M. Franco, Y. Pazos, B. Reguera, Evaluation of passive samplers as a monitoring tool for early warning of Dinophysis toxins in shellfish, Mar. Drugs. 11 (2013) 3823–3845, http://dx.doi.org/10.3390/md11103823.

[10] X. Feng, X. Ding, D. Jiang, Covalent organic frameworks, Chem. Soc. Rev. 41 (2012) 6010–6022, http://dx.doi.org/10.1039/c2cs35157a.

[11] S.-Y. Ding, W. Wang, Covalent organic frameworks (COFs): from design to applications, Chem. Soc. Rev. 42 (2013) 548–568, http://dx.doi.org/10.1039/c2cs35072f.

[12] U. Díaz, A. Corma, Ordered covalent organic frameworks, COFs and PAFs. From preparation to application, Coord. Chem. Rev. 311 (2016) 85–124, http://dx.doi.org/10.1016/j.ccr.2015.12.010.

[13] S. Kandambeth, A. Mallick, B. Lukose, M.V. Mane, T. Heine, R. Banerjee, Construction of crystalline 2D covalent organic frameworks with remarkable chemical (acid/base) stability via a combined reversible and irreversible route, J. Am. Chem. Soc. 134 (2012) 19524–19527, http://dx.doi.org/10.1021/ja308278w.

[14] S. Chandra, S. Kandambeth, B.P. Biswal, B. Lukose, S.M. Kunjir, M. Chaudhary, R. Babarao, T. Heine, R. Banerjee, Chemically stable multilayered covalent organic nanosheets from covalent organic frameworks via mechanical delamination, J. Am. Chem. Soc. 135 (2013) 17853–17861, http://dx.doi.org/10.1021/ja408121p.

[15] Q. Fang, Z. Zhuang, S. Gu, R.B. Kaspar, J. Zheng, J. Wang, S. Qiu, Y. Yan, Designed synthesis of large-pore crystalline polyimide covalent organic frameworks, Nat. Commun. 5 (2014) 4503, http://dx.doi.org/10.1038/ncomms5503.

[16] S.-B. Yu, H. Lyu, J. Tian, H. Wang, D.-W. Zhang, Y. Liu, Z.-T. Li, A polycationic covalent organic framework: a robust adsorbent for anionic dye pollutants, Polym. Chem. 7 (2016) 3392–3397, http://dx.doi.org/10.1039/c6py00281a.

[17] X. Zhu, S. An, Y. Liu, J. Hu, H. Liu, C. Tian, X. Yang, H. Wang, C.W. Abney, S. Dai, Efficient removal of organic dye pollutants using covalent organic frameworks, AIChE J. (2017), http://dx.doi.org/10.1002/aic.15699.

[18] S. Kandambeth, B.P. Biswal, H.D. Chaudhari, K.C. Rout, S. Kunjattu H, S. Mitra, S. Karak, A. Das, R. Mukherjee, U.K. Kharul, R. Banerjee, Selective molecular sieving in self-standing porous covalent-organic-framework membranes, Adv. Mater. 29 (2017) 1603945, http://dx.doi.org/10.1002/adma.201603945.

[19] Q. Fang, J. Wang, S. Gu, R.B. Kaspar, Z. Zhuang, J. Zheng, H. Guo, S. Qiu, Y. Yan, 3D porous crystalline polyimide covalent organic frameworks for drug delivery, J. Am. Chem. Soc. 137 (2015) 8352–8355, http://dx.doi.org/10.1021/jacs.5b04147.

[20] L. Bai, S.Z.F. Phua, W.Q. Lim, A. Jana, Z. Luo, H.P. Tham, L. Zhao, Q. Gao, Y. Zhao, Nanoscale covalent organic frameworks as smart carriers for drug delivery, Chem. Commun. 52 (2016) 4128–4131, http://dx.doi.org/10.1039/C6CC00853D.

[21] V.S. Vyas, M. Vishwakarma, I. Moudrakovski, F. Haase, G. Savasci, C. Ochsenfeld, J.P. Spatz, B.V. Lotsch, Exploiting noncovalent interactions in an imine-Based covalent organic framework for quercetin delivery, Adv. Mater. 28 (2016) 8749–8754, http://dx.doi.org/10.1002/adma.201603006.

[22] M.S. Lohse, T. Stassin, G. Naudin, S. Wuttke, R. Ameloot, D. De Vos, D.D. Medina, T. Bein, Sequential pore wall modification in a covalent organic framework for application in lactic acid adsorption, Chem. Mater. 28 (2016) 626–631, http://dx.doi.org/10.1021/acs.chemmater.5b04388.

[23] J.H. Chong, M. Sauer, B.O. Patrick, M.J. MacLachlan, Highly stable keto-enamine salicylideneanilines, Org. Lett. 5 (2003) 3823–3826, http://dx.doi.org/10.1021/ol0352714.

[24] S. Karak, S. Kandambeth, B.P. Biswal, H.S. Sasmal, S. Kumar, P. Pachfule, R. Banerjee, Constructing ultraporous covalent organic frameworks in seconds via an organic terracotta process, J. Am. Chem. Soc. 139 (2017) 1856–1862, http://dx.doi.org/10.1021/jacs.6b08815.

[25] J.D. Seader, E.J. Henley, Adsorption, ion change, and chromatography, in: Sep. Process Princ, 2nd ed., John Wiley {&} Sons, Inc., 2006, 2017, pp. 548–621.

[26] L. Fan, G. Sun, J. Qiu, Q. Ma, P. Hess, A. Li, Effect of seawater salinity on pore-size distribution on a poly(styrene)-based HP20 resin and its adsorption of diarrhetic shellfish toxins, J. Chromatogr. A 1373 (2014) 1–8, http://dx.doi.org/10.1016/j.chroma.2014.11.008.

[27] R. Apak, Adsorption of Heavy metal ions on soil surfaces and similar substances, in: A.T. Hubband (Ed.), Encycl. Surf. Colloid Sci., Vol. 1, Marcel Dekker, Inc, New York, 2002, pp. 385–417.

[28] Z. Chen, B. Xing, W.B. McGill, A unified sorption variable for environmental applications of the freundlich equation, J. Environ. Qual. 28 (1999) 1422–1428.

[29] P. Rodríguez, A. Alfonso, E. Turrell, J.-P. Lacaze, L.M. Botana, Study of solid phase adsorption of paralytic shellfish poisoning toxins (PSP) onto different resins, Harmful Algae. 10 (2011) 447–455, http://dx.doi.org/10.1016/j.hal.2011.02.005.

[30] G.P. Mashile, P.N. Nomngongo, Recent application of solid phase based techniques for extraction and preconcentration of cyanotoxins in environmental matrices, Crit. Rev. Anal. Chem. 47 (2017) 119–126, http://dx.doi.org/10.1080/10408347.2016.1225255.